Surrogate markers of intestinal dysfunction associated with survival in advanced cancers

Roxanne Birebent, Damien Drubay, Carolina Alves Costa Silva, Federica Marmorino, Giacomo Vitali, Gianmarco Piccinno, Yoan Hurtado, Adele Bonato, Lorenzo Belluomini, Meriem Messaoudene, Bertrand Routy, Marine Fidelle, Gerard Zalcman, Julien Mazieres, Clarisse Audigier-Valette, Denis Moro-Sibilot, François Goldwasser, Arnaud Scherpereel, Hervé Pegliasco, François Ghiringhelli, Anna Reni, Fabrice Barlesi, Laurence Albiges, David Planchard, Stéphanie Martinez, Benjamin Besse, Nicola Segata, Chiara Cremolini, Laurence Zitvogel, Valerio Iebba & Lisa Derosa

View supplementary material

Published online: 06 Apr 2025.

Submit your article to this journal

Article views: 4161

View related articles

Taylor & Francis
Taylor & Francis Group

ORIGINAL RESEARCH

 OPEN ACCESS   Check for updates

Surrogate markers of intestinal dysfunction associated with survival in advanced cancers

Roxanne Birebent[a,b,c*], Damien Drubay[a,d,e*], Carolina Alves Costa Silva[a,b,c*], Federica Marmorino[f,g*], Giacomo Vitali[a,c,h], Gianmarco Piccinno[i], Yoan Hurtado[a,b,c], Adele Bonato[a,c,f], Lorenzo Belluomini[a,c,j], Meriem Messaoudene[k,l], Bertrand Routy[k,l], Marine Fidelle[a,b,c], Gerard Zalcman[m], Julien Mazieres[n], Clarisse Audigier-Valette[o], Denis Moro-Sibilot[p], François Goldwasser[q,r,s], Arnaud Scherpereel[t], Hervé Pegliasco[u], François Ghiringhelli[v,w,x], Anna Reni[a,c,j], Fabrice Barlesi[a,b,y], Laurence Albiges[a,b,y], David Planchard[a,b,y], Stéphanie Martinez[z], Benjamin Besse[a,b,y], Nicola Segata[i,aa], Chiara Cremolini[f,g*], Laurence Zitvogel[a,b,c,bb*], Valerio Iebba[a,y*], and Lisa Derosa [ID][a,b,c,y*]

aGustave Roussy Cancer Campus, ClinicObiome, Villejuif, France; bFaculté de Medicine, Université Paris-Saclay, Ile-de-France, France; cInstitut National de la Santé et de la Recherche Médicale (INSERM) U1015, Equipe Labellisée-Ligue Nationale contre le Cancer, Villejuif, France; dOffice of Biostatistics and Epidemiology, Gustave Roussy Cancer Campus, Université Paris-Saclay, Villejuif, France; eInserm, Université Paris-Saclay, CESP U1018, Oncostat, Villejuif, France; fUnit of Medical Oncology 2, University Hospital of Pisa, Pisa, Italy; gDepartment of Translational Research and New Technologies in Medicine and Surgery, University of Pisa, Pisa, Italy; hMetaGenoPolis, INRAe, Université Paris-Saclay, Jouy en Josas, France; iDepartment CIBIO, University of Trento, Trento, Italy; jSection of Innovation Biomedicine - Oncology Area, Department of Engineering for Innovation Medicine (DIMI), University of Verona and University and Hospital Trust (AOUI) of Verona, Verona, Italy; kCentre Hospitalier de l'Université de Montréal (CHUM), Hematology-Oncology Division, Department of Medicine, Montréal, QC, Canada; lCentre de Recherche du CHUM (CRCHUM), Montréal, QC, Canada; mThoracic Oncology Department-CIC1425/CLIP2 Paris-Nord, Bichat-Claude Bernard Hospital, AP-HP, Université Paris Cité, Paris, France; nService de Pneumologie, Centre Hospitalier Universitaire de Toulouse, Toulouse, France; oPneumology Department, Centre Hospitalier Toulon Sainte-Musse, Toulon, France; pDepartment of Thoracic Oncology, Centre Hospitalier Universitaire, Grenoble, France; qINSERM U1016-CNRS UMR8104-Cochin Institute, Université Paris-Cité, Paris,France; rDepartment of Medical Oncology, Cochin Hospital, Assistance Publique-Hôpitaux de Paris, Paris, France; sImmunomodulatory Therapies Multidisciplinary Study Group (CERTIM), Paris, France; tDepartment of Pulmonary and Thoracic Oncology, University of Lille, University Hospital (CHU), INSERM unit OncoThAI, Lille, France; uPulmonary Department, European Hospital, Marseille, France; vCancer Biology Transfer Platform, Centre Georges-François Leclerc, Dijon, France; wCentre de Recherche INSERM LNC-UMR1241-CTM (Center of Translational and Molecular Medicine), Dijon, France; xDepartment of Medical Oncology, Centre Georges-François Leclerc, Dijon, France; yDepartment of Clinical Oncology, Gustave Roussy, Villejuif, France; zService des Maladies Respiratoires, Centre Hospitalier d'Aix-en-Provence, Aix-en-Provence, France; aaIEO, European Institute of Oncology IRCCS, Milan, Italy; bbCenter of Clinical Investigations in Biotherapies of Cancer (BIOTHERIS) 1428, Villejuif, France

ABSTRACT

Deviations in the diversity and composition of the gut microbiota are called "gut dysbiosis". They have been linked to various chronic diseases including cancers and resistance to immunotherapy. Stool shotgun based-metagenomics informs on the ecological composition of the gut microbiota and the prevalence of homeostatic bacteria such as *Akkermansia muciniphila (*Akk), while determination of the serum addressin MAdCAM-1 instructs on endothelial gut barrier dysfunction. Here we examined patient survival during chemo-immuno-therapy in 955 cancer patients across four independent cohorts of non-small cell lung (NSCLC), genitourinary (GU) and colorectal (CRC) cancers, according to hallmarks of gut dysbiosis. We show that Akk prevalence represents a stable and favorable phenotype in NSCLC and CRC cancer patients. Over-dominance of Akk above the healthy threshold was observed in dismal prognosis in NSCLC and GU and mirrored an immunosuppressive gut ecosystem and excessive intestinal epithelial exfoliation in NSCLC. In CRC, the combination of a lack of Akk and low sMAdCAM-1 levels identified a subset comprising 28% of patients with reduced survival, independent of the immunoscore. We conclude that gut dysbiosis hallmarks deserve integration within the diagnosis toolbox in oncological practice.

Introduction

Since the advent of immune checkpoint inhibitors (ICI), identifying biomarkers has become essential for better predicting resistance risks. The Food and Drug Administration has approved Expression of Programmed Cell Death Protein 1 (PD-L1) and tumor mutational burden for anti-Programmed Cell Death Protein 1 (PD-1)/PD-L1 antibodies. PD-L1 was predictive in

about 29% of trials, not predictive in 53.3% and not tested in 17.8% of the cases.[1]

Nine FDA approvals were linked to a specific PD-L1 threshold and companion diagnosis.[1] Cancer type, country, marker threshold, and methodology are key factors currently being validated to enhance biomarkers use in precision medicine.[2,3]

Other blood or tumor biomarkers, like myeloid-derived suppressor cells (MDSCs), circulating tumor cells (CTCs), CD8^{+} memory T-cells, T-cell receptor (TCR) diversity, tumor-infiltrating lymphocytes (TILs), and T-cell inflamed gene expression profiling, particularly in melanoma, also correlate with ICI response.[4] In addition, gut microbiota composition is increasingly recognized for its association with ICI clinical benefit across solid and hematological malignancies.[5–11]

Carcinogenesis, co-morbidities and co-medications (anti-biotics, proton pump inhibitors, laxatives, chemotherapy) influence the gut microbiota composition.[12–16] Studies on Gut OncoMicrobiome Signatures (GOMS) in meta-analyses reveal differences between cancer patients and healthy volunteers (HV), potentially aiding in the identification of responders from non-responders to ICI.[10] In particular, *Akkermansia muciniphila*[5,17] Lachnospiraceae (including *Roseburia spp., Coprococcus spp., Dorea spp.* among others), and Oscillospiraceae family members (such as *Faecalibacterium prausnitzii, R. bromii, R. bicirculans*) were associated with clinical benefit to ICI, while oral taxa (*Streptococcus spp., Veillonella spp., Actinomyces spp.), Hungatella hathewayi, Proteobacteria spp.* and the genus Enterocloster were associated with antibiotics[18] and/or ICI resistance.[10,19,19–22] The development of diagnostic tools for gut dysbiosis has been hampered by confounding factors affecting the consensual definition of clinically relevant GOMS. Technical considerations (sample collection, DNA extraction), patient geography, diet, lifestyle differences, varying clinical outcome parameters (e.g., objective response rate (ORR) versus progression-free (PFS) or overall survival (OS)) have limited the interpretation of microbial signals differentiating ICI responders from non-responders. Cancer type also contributes to discrepancies between studies.[5,7,19]

To minimize these confounding factors, we focused on advanced non-small cell lung cancer (NSCLC), renal cell carcinoma (RCC) and urothelial cancer (UC) which share GOMS,[5,17,18] in particular the immunogenic *Akkermansia muciniphila (*Akk) and two species interacting groups (SIG) of bacteria – one harmful (SIG1) and one beneficial (SIG2) for patient prognosis-, as summarized by a gut dysbiosis score (TOPOSCORE).[23] Another simple method to assess gut dysbiosis involves a gut-specific marker of endothelial barrier integrity, the soluble mucosal addressin cell adhesion molecule-1 (sMAdCAM-1).[24] Gut dysbiosis affects cancer immunosurveillance by, at least in part, decreasing expression of the endothelial counterpart MAdCAM-1 expression, as observed in the ileum after colonization by pathobionts such as *Enterocloster spp.* following antibiotic use[24] or tumor progression.[12] Since ileal MAdCAM-1 levels correlated with sMAdCAM-1 and deviated gut taxonomic composition, sMAdCAM-1 can serve as a reliable hallmark of gut dysbiosis and prognosis in NSCLC, RCC and UC patients treated with ICI.[24]

Here we analyzed the inter-relationship between these hallmarks of gut dysbiosis in 771 patients across 3 tumor subtypes extending these findings to 184 patients with metastatic colorectal cancer (CRC) treated with chemo-/+immunotherapy.

Methods

Study participant details

All patients provided written informed consent. GDPR and anonymization procedures were followed per Oncobiome H2020 at the ClinicoBiome, Gustave Roussy. Data and sample collection adhered to regulatory and ethical requirements and ICH E6(R2) Good Clinical Practice (GCP). Ancestry, race, ethnicity, socioeconomic were excluded due to France's Data Protection Act No. 78–17.

[https://www.advamed.org/sites/default/files/resource/112_112_code_of_ethics_0.pdf.]

Clinical trials and regulatory approvals

Oncobiotics

NCT04567446, is a multicenter study evaluating the microbiome impact on outcome in advanced NSCLC and RCC treated with anti-PD-(L)1therapies, alone or in combination with chemotherapy or tyrosine-kinase inhibitors. Conducted at 14 centers in France and Canada, the study followed standard care until disease progression, unacceptable side effects, or 2 years of ICI treatment. Eligibility criteria and baseline data, including recent medications, are in the trial protocol and recorded in electronic case reports.[23]

ATEZOTribe

The NCT03721653 phase 2 study enrolled 218 patients with unresectable stage IV CRC, randomized 2:1 to receive FOLFOXIRI+bevacizumab+atezolizumab (anti-PD-L1) or FOLFOXIRI+bevacizumab. At first stool collection, patients were treatment-naive. Baseline samples were available for 184 patients: 172 stools, 162 plasma and 150 had both. Samples collection followed ONCOBIOTICS cohort guidelines.[25]

IOPREDI/STRONG

NCT03084471, the French cohort of the STRONG phase IIIb trial,[26] treated bladder cancer patients, who progressed on chemotherapy, with durvalumab (150 mg every 4 weeks until progression). Baseline stool samples ($n = 133$) from AstraZeneca were used alone or pooled with the ONCOBIOTICS kidney cancer cohort.

Healthy volunteers

We used metagenomes of public databases (matched with cancer patients based on age, sex, and country) using the MetaPhlAn 4.0 pipeline as in.[23]

Metagenomic analyses

Stool samples underwent DNA extraction and sequencing via Ion Proton technology following MetaGenoPolis protocols. Gene abundance was assessed using human[27] and oral[28] microbiome catalogs, with reads mapped to the gene catalogs and normalized for sequencing depth (20 M). Metagenomics Species Pangenomes (MSP) were defined as clusters of co-abundant genes[29] with profiles merged from gut and oral catalogs. Metagenomic microbial

species (MGS) and strains were retrieved by means of MetaPhlAn4 (vJan21_CHOCOPhlAn)[30] which, after removal of genus-level genome bins (GGBs), eukaryotic microbes, and a 2.5% prevalence cutoff, retrieved a total of 601 species and 2649 species-level genome bins (SGBs).

Plasma sample processing and sMAdCAM-1 analyses

sMAdCAM-1 levels in plasma or serum samples were measured with a commercial kit from R&D Systems and read with the Bio-Plex 200 systems, as previously described.[24]

Clinical endpoints

Progression-free survival (PFS) was defined as time to progression or death and overall survival (OS) as the time to death, with patients censored at follow-up if no event occurred.

Statistical analyses

Microbial α (Shannon, richness metrics) and β diversity (Bray-Curtis dissimilarity) were analyzed using SciKit-learn v.1.6.1[31] under the Python v.3.8 environment. Inter-cohort comparisons were employed with ANOSIM and PERMANOVA tests after a proper batch-correction was performed with MMUPHin.[32] Discriminant species were identified via Partial Least Squared Discriminant Analysis coupled to Variable Importance (PLSDA-VIP). Survival analysis was performed using Kaplan-Meier curves, log-rank tests, and Cox regression, with significance defined as $p < 0.05$. For any biomarker that reached statistical significance, its predictive effect was assessed by examining its interaction with treatment. All analyses were conducted using R software (http://www.R-project.org/).

Results

Prevalence and clinical significance of fecal Akkermansia muciniphila in patients with advanced cancer

We analyzed data from our previous studies (NCT03084471), which included 499 NSCLC (1st or further therapy lines (L)) from France and Canada since 2017, 82 patients with RCC and 133 UC (1st L or further) in France[23] (Table S1). Moreover, we enrolled 57 NSCLC patients from the prospective IMMUNOLIFE1 study, not yet reported (Table S1) and data from the Phase II AtezoTRIBE trial, comparing chemoimmunotherapy (FOLFOXIRI+bevacizumab+atezolizumab) with chemotherapy alone (FOLFOXIRI+bevacizumab) in metastatic CRC patients (Table S1).[25,33] Among 955 patients, 943 stool samples were available before ICI initiation, allowing shotgun metagenomics (MGS) analysis defining microbiota composition (Table S2).

In a previous study of 338 NSCLC patients, we found that intestinal colonization with Akkermansia muciniphila was associated with increased ORR and OS.[17] We extended this analysis to include new cohorts, and we examined the prevalence of three Akkermansia spp. (SGB9224, SGB9226 and SGB9228) using MetaPhlAn4 profiling across all cancer histotypes versus healthy volunteers.[34] As previously reported, Akkermansia muciniphila SGB9226 (Akk9226) was the most prevalent species, followed by Akkermansia massiliensis SGB9228 (Akk9228) and Akkermansia biwaensis SGB9224 (Akk9224).[35] Notably, the prevalence of distinct SGB may vary by cancer type, with SGB9228 slightly more prevalent in urinary cancer (Table 1 , Figure 1a).

To assess the stability of the most prevalent phenotype, the presence of intestinal Akk9226, we performed a longitudinal MGS follow-up on 141 NSCLC patients with 282 paired stools over time. Within 3 months, 9% (7/78) of Akk9226 negative (Akk9226^{Neg}) became positive (Akk9226^{Pos}) or vice versa in 17% (11/63) cases. Over 6 months or more, 17% of Akk9226^{Neg} (11 + 2/78) became Akk9226^{Pos} and 14% (5 + 4/63) of Akk9226^{Pos} became Akk9226^{Neg}. Overall, the Akk9226 phenotype remained relatively stable during the first 3 months of ICI treatment and eventually evolved with treatment response (Figure 1b) .

We confirmed our initial observation in a larger cohort of 556 NSCLC patients, whereby the absence of gut Akk9226 at baseline was linked to a dismal prognosis in univariable analysis (Figure 2a, HR: 0.78 (0.61–0.98), $p = 0.033$, Table S2A) and tended to be associated with poor prognosis in multivariable analysis, mostly for 2nd L patients (Table S3A, HR: 0.80 (0.63–1.03), $p = 0.078$).

In CRC patients, similar results were observed for Akk9226 in univariable analysis (Figure 2b, HR: 0.63 (0.42–-0.95), $p = 0.028$), yet not in multivariable analysis (not shown, $p = 0.315$). Conversely, the absence of Akk9226 at baseline was not associated with OS in both RCC and UC, either individually or combined (GU) (Figure 2c, GU-HR: 0.96

Table 1. Prevalence and relative abundances of three species of Akkermansia in study cohorts.

Cohort	n	Akk9226 Prevalence, n (%)	Akk9226 Mean (%)* SD	Akk9228 Prevalence, n (%)	Akk9228 Mean (%)* SD	Co-colonized Akk9226 & Akk9228 Prevalence, n (%)	Absence Akk9226 & Akk9228 Prevalence, n (%)	Akk9224 Prevalence, n (%)	Akk9224 Mean (%)* SD
HV	124	62 (50)	1 ± 1.5	12 (9.7)	1.4 ± 1.5	7 (5.6)	57 (46)	4 (3.2)	1.6 ± 2.6
NSCLC	556	271 (48.7)	3.1 ± 6.8	60 (10.8)	3.6 ± 8.3	27 (4.9)	252 (45.3)	9 (1.6)	1.4 ± 2.2
France	471	233 (49.5)	3.2 ± 6.9	47 (10)	2.7 ± 6.0	21 (4.5)	212 (45)	6 (1.3)	1.7 ± 2.6
Canada	85	38 (44.7)	2.6 ± 6.0	13 (15.3)	6.9 ± 13.6	6 (7.1)	40 (47.1)	3 (3.5)	0.6 ± 0.8
UC	133	61 (45.9)	2.4 ± 3.9	20 (15)	3.3 ± 5.3	1 (0.8)	53 (39.8)	4 (3)	4.6 ± 6.8
RCC	82	45 (54.9)	1.7 ± 2.6	7 (8.5)	3.5 ± 4.2	3 (3.7)	33 (40.2)	3 (3.7)	0.4 ± 0.4
CRC	172	81 (47.1)	3.7 ± 5.4	10 (5.8)	4.1 ± 4.5	2 (1.2)	83 (48.3)	5 (2.9)	1.9 ± 2.5

considering only Akk^{Pos} patients.
HV: Healthy volunteers.
NSCLC: Non-small cell lung cancer.
UC :Urothelial cancer.
RCC : Renal cell carcinoma.
CRC: colorectal cancer.
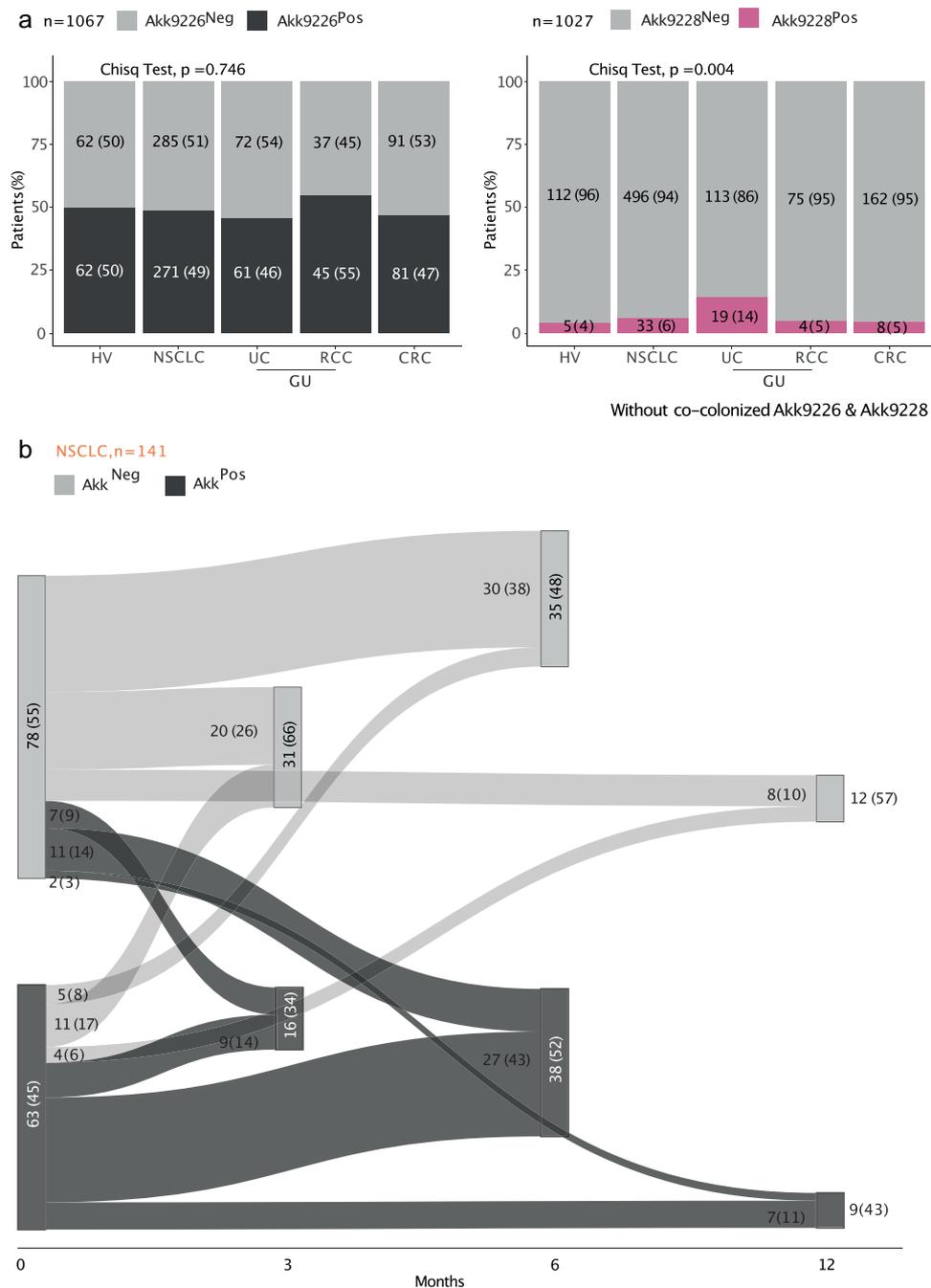Standard deviation (SD) quantifies the amount of variation.

Figure 1. Prevalence of *Akkermansia spp.* in cancer patients and matched healthy volunteers (HV). a. Stool prevalence of Akk9226 (left) and 9228 (right) in cancer patients and sex and age matched French HV. b. Sankey diagram showing Akk prevalence (either 9226 and/or Akk9228) prevalence over time in paired specimens from 141 NSCLC patients followed longitudinally.

(0.68–1.34), $p = 0.792$; UC-HR: 1.13 (0.79–1.74), $p = 0.594$; RCC-HR: 0.98 (0.57–1.67), $p = 0.935$). Interestingly, when examining the compositional taxonomic differences in the gut microbiota of CRC patients segregated between Akk9226[Pos] and Akk9226[Neg], we found a significant increase in alpha-diversity monitored using the Shannon ($p = 0.044$) and richness ($p = 0.0034$) metrics in Akk9226[Pos] CRC patients (Figure S1A), as well as differences in the overall taxonomic composition between both groups (Figure S1B). Following PLSDA-VIP analysis, we found an overabundance of Oscillospiraceae and Lachnospiraceae family members in

Akk9226[Pos] stools as previously reported,[17] while feces from Akk9226[Neg] patients were overabundant in the genus Klebsiella (*K. michiganensis* and *K. pneumoniae)* (Figure S1C) which have been extensively described as drug-resistant[36] and pro-inflammatory[37] bacteria.

In contrast to Akk9226, the presence of Akk9228 alone (excluding the 5% of double-positive patients, Table 1, Figure 1a right panel) did not confer a favorable prognostic value in NSCLC (Figure S2). However, the rare prevalence of Akk9228 limits the statistical power of this analysis across different cancer types (Figure S2).
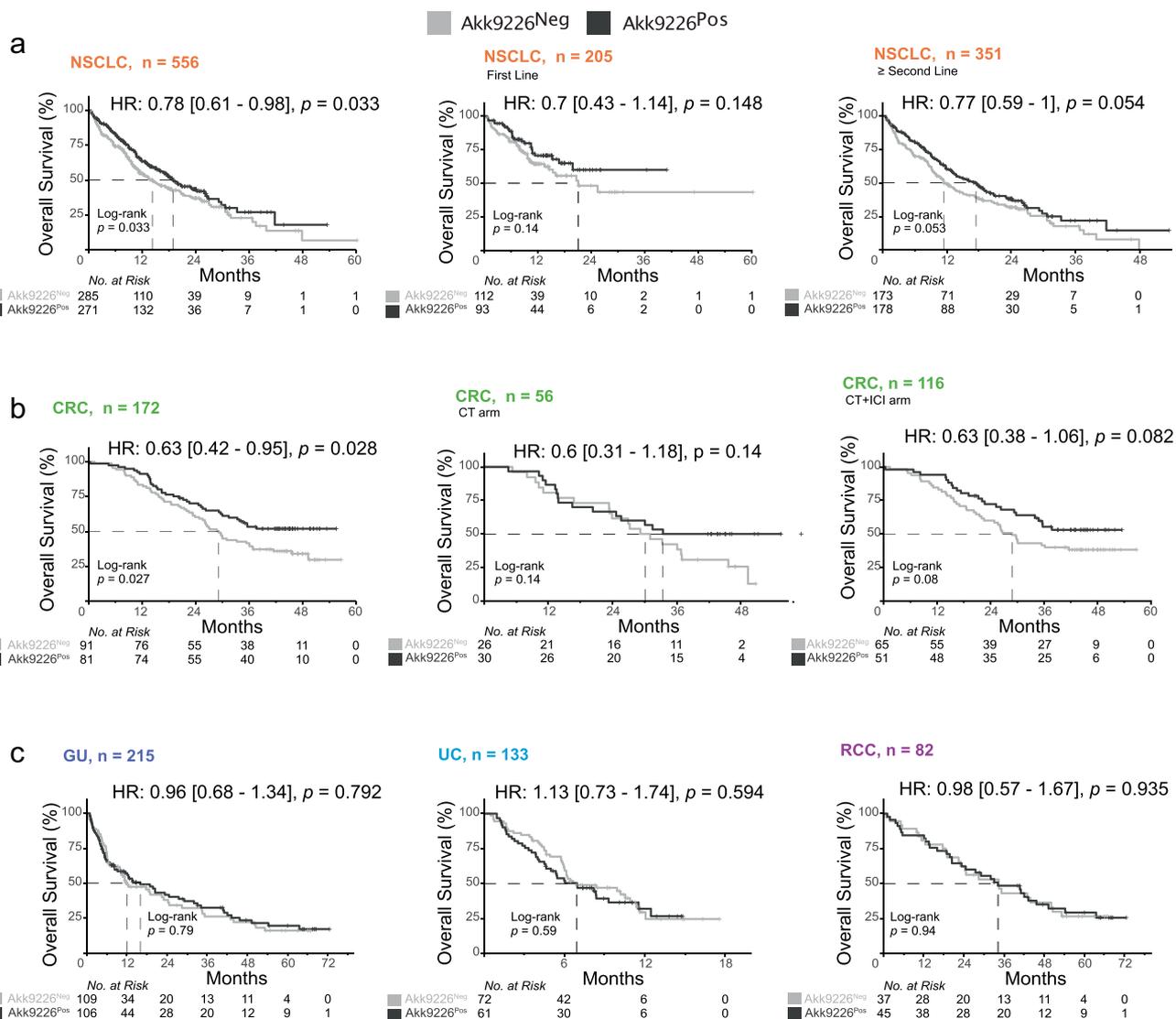
Figure 2. Prevalence of Akk9226 is associated with clinical benefit to therapies in NSCLC and CRC. Kaplan-Meier curves and Cox regression analyses of OS. A. NSCLC n = 556 by Akk9226 prevalence (left), 1st L of treatment (middle), 2nd line (right). See Table S3A for multivariable analyses. B. CRC n = 172 by Akk9226 status (left); chemotherapy n = 56 (middle), chemo-immunotherapy n = 116 (right). C. GU n = 215, including UC (n = 133, middle), RCC (n = 82, right), by Akk9226 status. Between groups, survival comparisons were performed using the two-sided log-rank test. The hazard ratios correspond to the related univariable Cox regression analyses. The conclusions were similar in the multivariable (also refer to Table S3A) p = 0.071.

Altogether, a deficit in gut Akk9226 is a poor prognostic factor in NSCLC and CRC, where it is associated with intestinal pathobionts and inflammatory bacteria.

High relative abundance of Akk9226 is associated with gut dysbiosis in NSCLC and GU

Based on our previous report on 338 NSCLC patients [17] showing that overabundance of Akk. spp. (exceeding the >4.799%, the 77%ile) conferred primary resistance to immunotherapy in NSCLC,[17] we next analyzed OS and PFS in the three groups stratified according to the relative abundance Akk9226. Of note, among bacteria with >2.5% prevalence, only Akk9226 displayed a trichotomic distribution, with both Akk9226^{Neg} and Akk9226^{High} correlating with dismal prognosis.[23] Here, 9% (48/556) of NSCLC patients exhibited Akk9226^{High} (Figure 3a). This phenotype, albeit not influencing PFS (p = 0.1), conferred a significant reduction in OS (p =

0.0019) compared to Akk9226^{Low} in first (p = 0.065) or further lines of therapy (p = 0.016) (Figure 3b–e) in uni- and multivariate analysis (Table S3B, HR:1.79 (1.18–2.73), p = 0.007) in NSCLC.

Previous work stated that lower richness or higher alpha diversity correlated with reduced ORR in metastatic melanoma patients.[6] To investigate whether high relative abundance of Akk9226 was an indirect proxy of a more complex gut dysbiosis, we next computed the taxonomic alpha and beta diversity of NSCLC patient stools in the three groups (Akk^{Neg}, Akk^{Low}, Akk^{High}) using the MetaPhlAn4 pipeline. A significant drop in the richness of the microbial ecosystem was observed in Akk9226^{Neg} compared with Akk9226^{Pos} patients and in Akk922^{High} patients versus Akk9226^{Low} patients (Figure 4a). Abnormal Akk9226^{Neg} or Akk9226^{High} ecosystems contained a relative over-representation of species from the immunosuppressive genus Enterocloster (E. aldensis, E. clostridioformis,
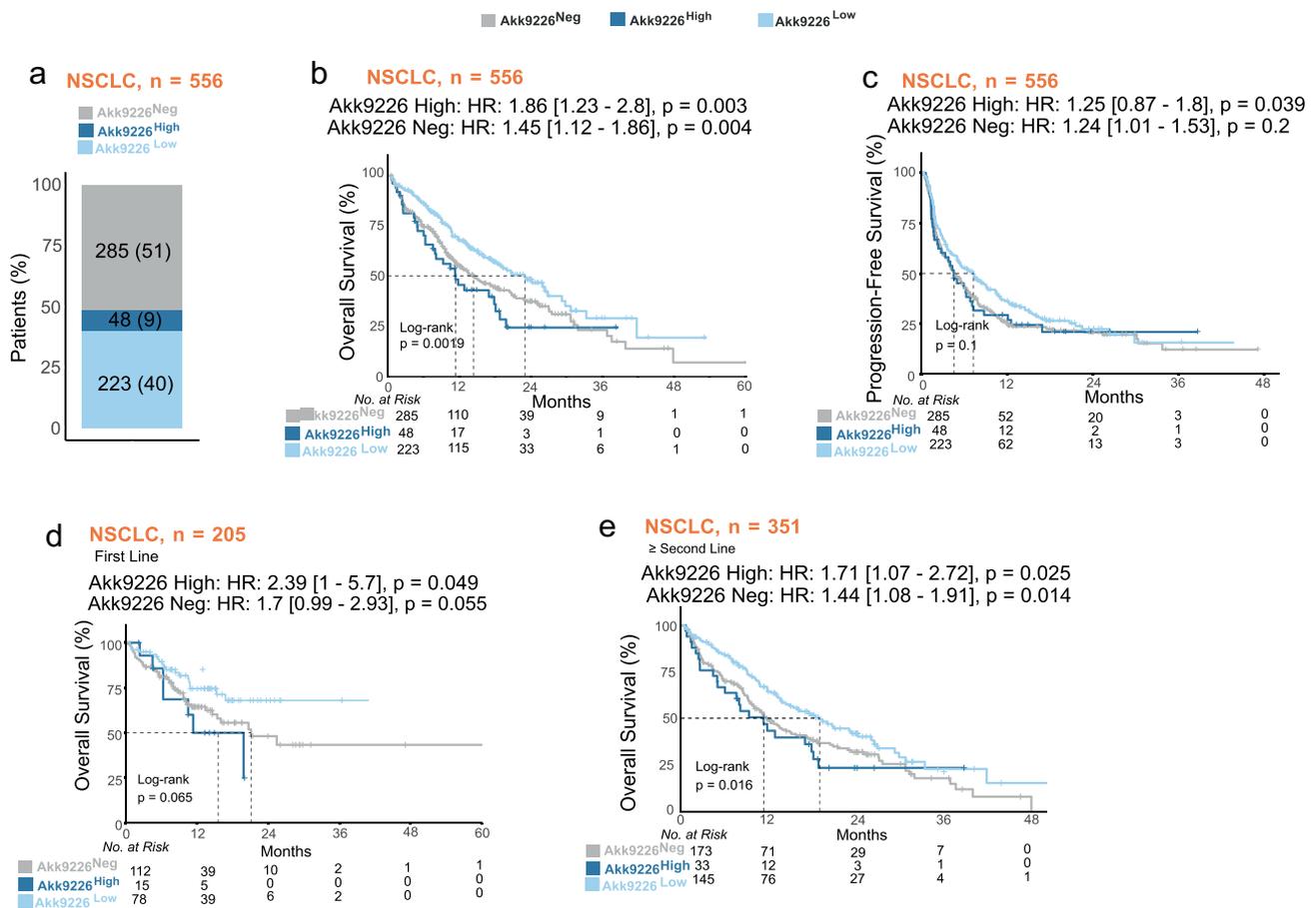
Figure 3. Low levels of Akk9226 are associated with favorable prognosis in NSCLC. A. Distribution of Akk9226 relative abundance in NSCLC patients: Akk9226Neg (undetectable), Akk9226Low (0–4.799%), Akk9226High (>4.799%). B-C. Kaplan-Meier curves and Cox model for OS (B) and PFS (C) in 556 NSCLC patients by Akk9226 status. D-E. Same for 1st L (D) and 2nd L (E) ICI in NSCLC. Between groups, survival comparisons were performed using the two-sided log-rank test. The hazard ratios correspond to the related univariable Cox analyses. The conclusions were similar in the multivariable (also refer to Table S3B, $p = 0.014$ vs Akk9226Neg and $p = 0.007$ vs Akk9226High).

E. bolteae), bacteria related to antibiotics usage (*Clostridium symbosium*, *C. scindens*) and immunoresistance to ICI (*Anaerostipes caccae*, *Blautia producta*)[23] (Figure 4a). We could extend these conclusions when admixing these 556 NSCLC patient stool metagenomics with that of 82 RCC and 133 UC subjects (total $N = 771$ patients). A significant drop in the richness of the microbial ecosystem was observed in Akk9226Neg compared with Akk9226Pos patients and in Akk922High patients versus Akk9226Low patients (Figure S3A). In addition, beta-diversities revealed distinct intestinal ecosystems among these three patients' groups (Figure S3B), suggesting different taxonomic compositions that were further analyzed with PLSDA-VIP (Figure S3C). Akk9226Neg or Akk9226High ecosystems differed significantly from Akk9226Low health-related microbiota, with a relative over-representation of species from the SIG1 group[23] (*Clostridium symbosium*, *F. plautii*, *Anaerostipes caccae*, *Limosilactobacillus fermentum*, and *Blautia producta*) and immunosuppressive genus Enterocloster (*E. aldensis*, *E. bolteae*, *E. clostridioformis*) (Figure S3C).

We then focused on the "exfoliome", originally described in a melanoma cohort,[19] where noninvasive transcriptomics of shed intestinal epithelial cells were analyzed in fecal samples.

Here, we extended this concept to stool DNA sequencing by calculating the contamination of prokaryotic DNA by mammalian eukaryotic DNA, establishing the ratio between the number of human reads and the total number of reads in each sample. We observed that this exfoliation was more pronounced in abnormal Akk9226Neg or Akk9226High ecosystems compared with normal Akk9226Low microbiota, mostly for 2nd L patients (Figure 4b), suggesting that dysbiosis accompanies epithelial barrier dysfunction.

Next, we studied the clinical relevance of abnormal Akk9226 relative abundances in the other cohorts of solid cancers. The proportion of Akk9226High (exceeding the >4.799%) patients was between 9% and 12%, significantly higher than that of healthy volunteers (Figure 5a, Table S2B). The Cox regression analysis of GU malignancies corroborated the result obtained in NSCLC patients (Figure 5b, $p = 0.0056$). In both RCC and UC patients, albeit not significant because of size effect, the Akk9226High stool phenotype conferred shorter OS ($p=0.0011$ for UC and $p=0.47$ for RCC) but did not affect PFS ($p=0.11$ for UC and $p=0.22$ for RCC, Figure S4A-B). Contrasting with other cancer histotypes, the proportions of Akk9226High were higher in CRC patients and tended to convey a favorable prognosis (Figure 5c, $p = 0.073$).
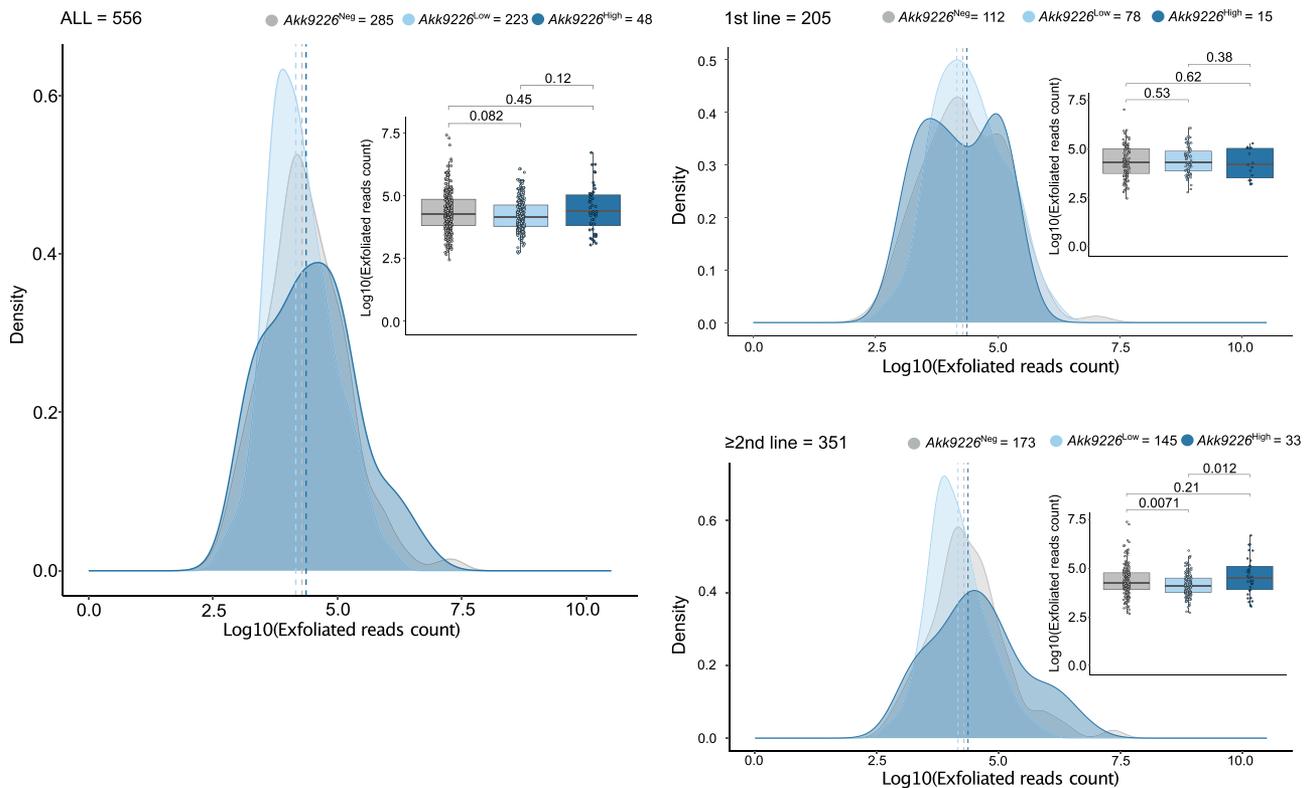
Figure 4. High Akk9226 relative abundance is a surrogate hallmark of gut dysbiosis and epithelial exfoliation. A. PCoA of fecal taxonomic composition (inset), Shannon and richness indices and VIP score for Akk9226Neg versus Akk9226Low (left) and Akk9226Low versus Akk9226High (right). ANOSIM and PERMANOVA assess group separation significance after 999 permutations. PLS-DA and VIP identify key microbial species by importance with bar color depicting the cohort with the highest mean relative abundance. Mann-Whitney test for significance (*$p < 0.05$, **$p < 0.01$, ***$p < 0.001$). B. Kernel density plot of the exfoliated human reads (Log10 scale) in three Akk9226 groups according to lines of therapy in NSCLC and significance between medians was computed with Kruskal-Wallis's test and Dunn's test.

Figure 5. High levels of Akk9226 are associated with dismal prognosis in urinary tract cancers (GU) but not CRC. a distribution of Akk9226 relative abundance in HV, GU and CRC patients: Akk9226^{Neg} (undetectable), Akk9226^{Low} (0–4.799%), Akk9226^{High} (>4.799%). P-value are fisher exact test with FDR correction. b, c. Kaplan-Meier curves and Cox model for OS in 215 GU patients (b) and 172 CRC patients (c) by Akk9226 status (Akk9226^{Neg}, Akk9226^{Low}, and Akk9226^{High}). Between groups, survival comparisons were performed using the two-sided log-rank test. The hazard ratios correspond to the related univariable Cox analyses.

Altogether, GU or NSCLC patients presenting Akk9226 relative abundances superior to >4.799% exhibit reduced OS compared with patients harboring normal pretreatment Akk9226 levels.

Coordinated defects in sMAdCAM-1 and Akk are risk factors for shorter survival in CRC

We previously found that higher plasma sMAdCAM-1 levels were associated with favorable prognosis in NSCLC, RCC and UC cancers.[24] We stratified patients based on Akk9226 (Pos versus Neg) and sMAdCAM-1 levels (≥ or < median, sMAdCAM^{High} or sMAdCAM^{Low} respectively) in each cancer type and found no clear association between their distribution, suggesting independent prognostic values (Figure S5A-C, Figure S6A-B). Moreover, Cox regression analyzes taking into account the two variables did not show any significant impact on PFS and OS in NSCLC (Figure S6A) or UC patients (Figure S6B).

However, again, the exception tended to be CRC where we observed a higher proportion of sMAdCAM-1^{High} within the Akk9226^{High}patients (32.4% in CRC vs 9.1% and 6.5% in UC and NSCLC, respectively, $\chi^2 = 4.72$, $p = 0.094$, not shown), further supporting the distinct significance of Akk9226^{High} in this cancer type. We evaluated sMAdCAM-1 in the AtezoTRIBE CRC cohort and found no significant differences in the two treatment arms at baseline (Figure 6a). As reported in other solid cancers, higher sMAdCAM-1 levels were associated with better OS in CRC, in univariable (Figure 6b, HR: 0.53 (0.35–0.8), $p = 0.0021$) in the whole cohort and in each treatment arm (Figure 6c, HR: 0.54 (-0.27–1.06), $p = 0.071$ in chemotherapy, HR: 0.53 (0.32–0.9), $p = 0.018$ in chemo-immunotherapy). However, the combination of sMAdCAM-1^{Low} and Akk^{Neg} identified a subgroup of 28% patients with a dismal prognosis for OS ($p < 0.001$, Figure 6d) and, to some extent, for PFS ($p = 0.21$, Figure 6e). The multivariable analysis confirmed sMAdCAM-1^{Low} as an independent risk factor when combined with Akk^{Neg} (Table S4, HR: 2.05 (1.28–3.30), $p =$

0.003), compared to patients with sMAdCAM-1^{High} or those with sMAdCAM-1^{Low} and either Akk^{Low} or Akk^{High}. Independently of sMAdCAM-1 and Akk variables, a high immunoscore identified a subset of favorable outcomes, but only in the chemoimmunotherapy arm (Table S4, HR: 0.24 (0.09–0.60), $p = 0.002$). In other words, an interaction between chemoimmunotherapy arm and Immunoscore was observed, as previously described,[33] but not with sMAdCAM-1 nor Akk levels.

Altogether, advanced CRC patients could be stratified not only based on the immunoscore, but also on gut biomarkers (Akk, sMAdCAM-1) for guide future interventions and optimize therapeutic strategies.[38]

Discussion

This work highlights the negative impact of gut microbiota imbalances on the clinical outcome of advanced cancer patients and the potential of gut-related surrogate biomarkers or "intestinal dysbiosis" to stratify patients in the chemo-immunotherapy regimen. We dedicated a special focus to distinct microbial species at the strain level as simple proxies for dysbiosis given their potential therapeutic role as live biotherapeutics.

Here we confirmed in 556 NSCLC patients that the absence of *Akkermansia muciniphila SGB9226* (49.5%) confers shorter survival, while 9% exhibiting an Akk9226^{High} phenotype presented a deviated repertoire of the gut microbiota associated with exacerbated epithelial exfoliation culminating in increased death rates.

A. muciniphila ("MucT") is under-represented in overweight individuals, linking its deficiency to metabolic disorders like obesity, Type 2 diabetes (T2D), nonalcoholic fatty liver disease and cardiovascular diseases.[39,39–43] Cani's group explored these connections in rodents and in T2D/obese patients in Microbes4U© study.[44] Daily administration of pasteurized MucT in mice reversed fat-mass gain, metabolic endotoxaemia, adipose tissue inflammation, reduced cholesterol levels and serum triglyceride levels and insulin resistance.[41,45]
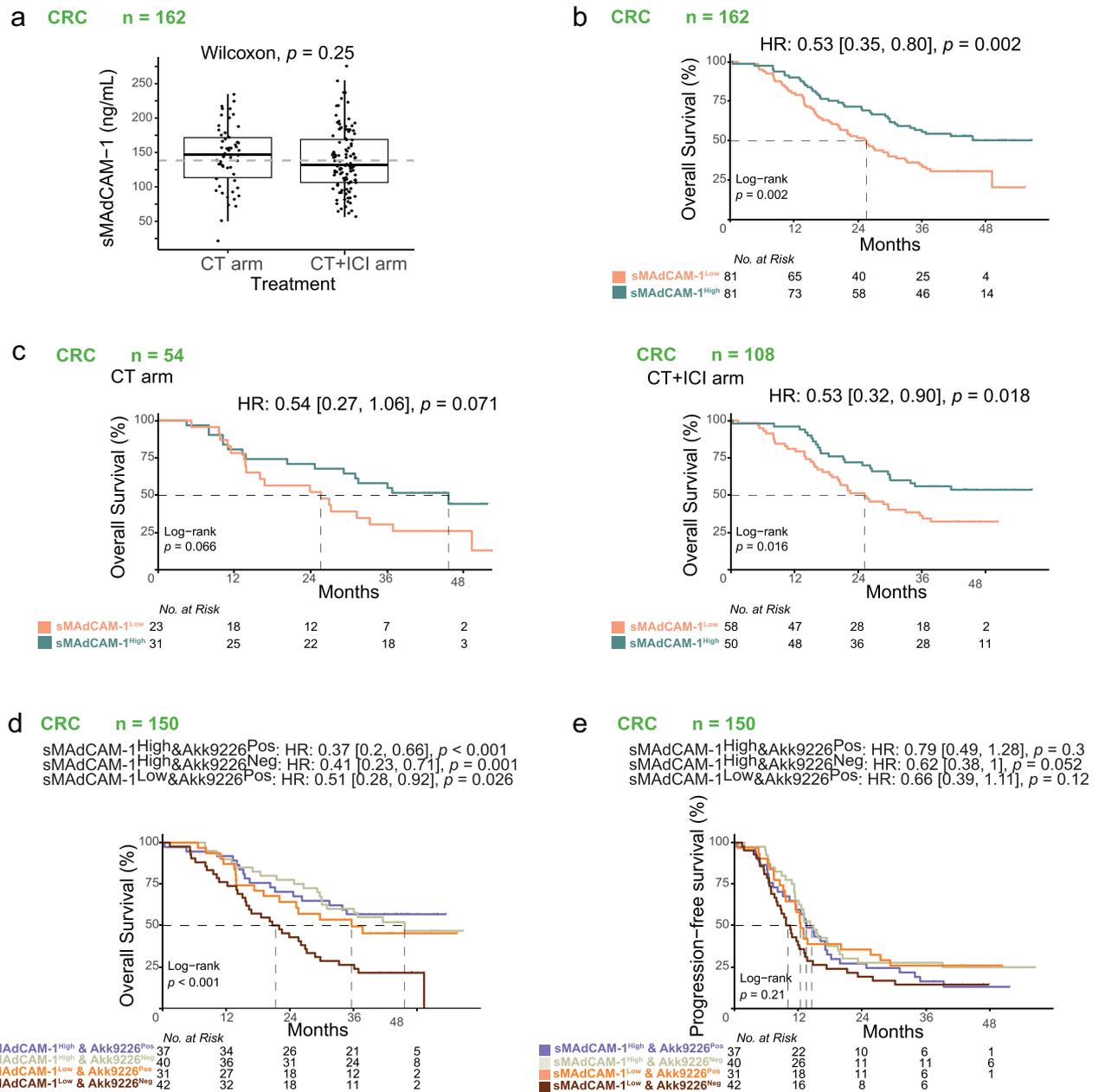
Figure 6. Interaction between sMadCAM-1 and Akk9226 as a prognostic signature in CRC. a. Plasma sMadCAM-1 levels by treatment arm in CRC. Each dot is one patient/plasma. b-c. Kaplan-Meier curves and multivariable Cox model for OS in CRC $n = 162$, in chemotherapy $n = 54$ (C, left) and in chemo-immunotherapy $n = 108$ (C, right) by sMadCAM-1 levels according to the cohort median (Low≤s138.4803 ng.mL^{-1}). d-e. Kaplan-Meier curves and Cox model for PFS (D) and OS (E) in 150 patients with paired stool and plasma samples according to sMadCAM-1 levels and Akk9226 prevalence (sMadCAM-1^{Low} or ^{High}, Akk9226^{Pos} or Akk9226^{Neg}). Between groups, survival comparisons were performed using the two-sided log-rank test. The hazard ratios correspond to the related univariable Cox analyses.

Restoring *A. muciniphila* levels also reduced the severity of viral infections,[46] inflammatory bowel and alcoholic liver diseases, colitis-associated tumorigenesis and progeria in mice.[47–50] A proof-of-concept study with 40 patients, showed that pasteurized, but not alive, MucT (10^{10} cells per day for 3 months) markedly improved insulin sensitivity and cholesterol levels, altered metabolic profiles, and promoted lipid beta-oxidation. It did not modulate the taxonomic composition of the microbiota.[44,51] This pioneering and successful trial using this food supplement in metabolic disorders paves the way to the development of live biotherapeutics as potential drugs to be applied in the subset of cancer patients

lacking endogenous *A. muciniphila*. A Phase I trial is currently underway at Gustave Roussy (NCT05865730) aimed at compensating Akk9226^{Neg} and Akk9228^{Neg} double-negative patients (45% cases in NSCLC, Table 1) with an immunogenic strain of *Akkermansia* p2261 **(named Oncobax®_AK)** to address this question in RCC and NSCLC.

The deleterious association between Akk9226^{High} and dismal outcome in NSCLC was extended to GU malignancies. The stool Akk^{High} phenotype most likely does not reflect cell intrinsic biological dysfunction of Akk, as exemplified by passive transfer of FMT Akk^{High} in avatar tumor bearers that failed to confer resistance to ICI, but rather a consequence of

a profound gut barrier dysfunction in the cancer patient leading to a protracted and severe intestinal dysbiosis.[12,17] Indeed, Akk[High] NSCLC and RCC patients displayed a similar taxonomic profile observed in SIG1 or antibiotics-treated patients dominated by Enterocloster and oral taxa mediating tolerogenic effects.[23,52] In CRC patients, where 12% are Akk9226[High] and 53% Akk9226[Neg], only patients with Akk9226[Neg] exhibited a reduced overall survival. This may be due to distinct microbiota and biofilms associated with the colon tumorigenesis,[53] and/or to a relative loss of health-associated bacteria such as Christensenellaceae, Oscillospiraceae, Lachnospiraceae family members.[54]

The shedding of MAdCAM-1, first described 20 years ago, occurs in the gut lymphoid tissues but also in the liver (in humans but not in mice).[55] It can be upregulated by inflammatory signals like TNFα, beta7 integrins, and vascular adhesion protein 1 (VAP-1). Methylamine (from food and cigarette smoke) could synergize with TNFα to promote MAdCAM-1 shedding *in vitro*.[55] In tumor-bearing mice, secondary bile acids (like lithocholic acid (LCA) and ursodeoxycholic acid (UDCA) downregulate ileal MAdCAM-1,[24] potentially affecting ICI efficacy. Recent studies unveiled that Farnesoid X receptor (FXR) signaling influenced by biliary acids impacts T cell functions and clinical outcomes in graft-versus-host disease (GVHD).[56] Chenodeoxycholic acid (CDCA) stimulated T cell activation, while UDCA inhibited it, paving the way to the potential efficacy of UDCA to reduce alloreactivity-related death rates during allogeneic hematopoietic stem cell transplantation.[57,58] While FXR inhibition reduces GVHD, it is tempting to speculate that FXR activation could enhance ICI effects in settings of gut dysbiosis or low MAdCAM-1. Low levels of sMAdCAM-1 in advanced NSCLC, RCC and UC were associated with poor survival despite immunotherapy.[24] This result is now extended to 1st line metastatic CRC, as depicted in this manuscript. What causes ileal MAdCAM-1 loss and/or shedding in the circulation remain an open conundrum. While *Akkermansia* sp2261 could maintain or upregulate ileal MAdCAM-1 expression in tumor bearing mice,[24] prevalence or relative abundance of Akk9226 did not coincide with higher sMAdCAM-1 in our cohorts.

Altogether, precision oncology could benefit from gut-derived biomarkers to improve immunotherapy trial design alves.[59] Stratifying patients based on gut dysbiosis markers (Akk prevalence, sMAdCAM-1, S score/Toposcore) at baseline may help identify those individuals deemed to fail immunotherapy and suitable for microbiota-centered interventions, such as live biotherapeutics, fecal microbiota transplant (FMT), and possibly distinct bile acids.

Acknowledgments

Disclosure statement

Funding

ORCID

Lisa Derosa http://orcid.org/0000-0003-0527-2964

References

1. Davis AA, Patel VG. The role of PD-L1 expression as a predictive biomarker: an analysis of all US food and drug administration (FDA) approvals of immune checkpoint inhibitors. J Immunother Cancer. 2019;7(1):278. doi: 10.1186/s40425-019-0768-9.

2. Sha D, Jin Z, Budczies J, Kluck K, Stenzinger A, Sinicrope FA. Tumor mutational burden as a predictive biomarker in solid tumors. Cancer Discov. 2020;10(12):1808–1825. doi: 10.1158/2159-8290.CD-20-0522.

3. Nassar AH. Ancestry-driven recalibration of tumor mutational burden and disparate clinical outcomes in response to immune checkpoint inhibitors. Cancer Cell. 2022;40:1161–1172.e5.

4. Baltussen JC, Welters MJP, Verdegaal EME, Kapiteijn E, Schrader AMR, Slingerland M, Liefers G-J, van der Burg SH, Portielje JEA, de Glas NA. Predictive biomarkers for outcomes of immune checkpoint inhibitors (ICIs) in melanoma: a systematic review. Cancers (Basel). 2021;13(24):6366. doi: 10.3390/cancers13246366.

5. Routy B, Le Chatelier E, Derosa L, Duong CPM, Alou MT, Daillère R, Fluckiger A, Messaoudene M, Rauber C, Roberti MP, et al. Gut microbiome influences efficacy of PD-1-based immunotherapy against epithelial tumors. Science. 2018;359 (6371):91–97. doi: 10.1126/science.aan3706.

6. Gopalakrishnan V, Spencer CN, Nezi L, Reuben A, Andrews MC, Karpinets TV, Prieto PA, Vicente D, Hoffman K, Wei SC, et al. Gut microbiome modulates response to anti–PD-1 immunotherapy in melanoma patients. Science. 2018;359(6371):97–103. doi: 10.1126/science.aan4236.

7. Matson V, Fessler J, Bao R, Chongsuwat T, Zha Y, Alegre M-L, Luke JJ, Gajewski TF. The commensal microbiome is associated with anti–PD-1 efficacy in metastatic melanoma patients. Science. 2018;359(6371):104–108. doi: 10.1126/science.aao3290.

8. Daillère R, Derosa L, Bonvalet M, Segata N, Routy B, Gariboldi M, Budinská E, De Vries IJM, Naccarati AG, Zitvogel V, et al. Trial watch: the gut microbiota as a tool to boost the clinical efficacy of anticancer immunotherapy. Oncoimmunology. 2020;9(1). doi: 10.1080/2162402X.2020.1774298.

9. Park EM, Chelvanambi M, Bhutiani N, Kroemer G, Zitvogel L, Wargo JA. Targeting the gut and tumor microbiota in cancer. Nat Med. 2022;28(4):690–703. doi: 10.1038/s41591-022-01779-2.

10. Thomas AM, Fidelle M, Routy B, Kroemer G, Wargo JA, Segata N, Zitvogel L. Gut OncoMicrobiome Signatures (GOMS) as next-generation biomarkers for cancer immunotherapy. Nat Rev Clin Oncol. 2023;20(9):583–603. doi: 10.1038/s41571-023-00785-8.

11. Stein-Thoeringer CK, Saini NY, Zamir E, Blumenberg V, Schubert M-L, Mor U, Fante MA, Schmidt S, Hayase E, Hayase T, et al. A non-antibiotic-disrupted gut microbiome is associated with clinical responses to CD19-CAR-T cell cancer immunotherapy. Nat Med. 2023;29(4):906–916. doi: 10.1038/s41591-023-02234-6.

12. Yonekura S, Terrisse S, Alves Costa Silva C, Lafarge A, Iebba V, Ferrere G, Goubet A-G, Fahrner J-E, Lahmar I, Ueda K, et al. Cancer induces a stress ileopathy depending on β-adrenergic receptors and promoting dysbiosis that contributes to carcinogenesis. Cancer Discov. 2021;12(4):1128–1151. doi: 10.1158/2159-8290.CD-21-0999.

13. Terrisse S. Intestinal microbiota influences clinical outcome and side effects of early breast cancer treatment. Cell Death Differ. 2021; 1–19. doi: 10.1038/s41418-021-00784-1.

14. Terrisse S, Goubet A-G, Ueda K, Thomas AM, Quiniou V, Thelemaque C, Dunsmore G, Clave E, Gamat-Huber M, Yonekura S, et al. Immune system and intestinal microbiota determine efficacy of androgen deprivation therapy against prostate cancer. J Immunother Cancer. 2022;10(3):e004191. doi: 10.1136/jitc-2021-004191.

15. Roberti MP. Chemotherapy-induced ileal crypt apoptosis and the ileal microbiome shape immunosurveillance and prognosis of proximal colon cancer. Nat Med. 2020;26:919–931.

16. Derosa L. Microbiota-centered interventions: the next breakthrough in immuno-oncology? Cancer Discov. 2021;11:2396–2412.

17. Derosa L. Intestinal Akkermansia muciniphila predicts clinical response to PD-1 blockade in patients with advanced non-small-cell lung cancer. Nat Med. 2022; doi: 10.1038/s41591-021-01655-5.

18. Derosa L. Gut bacteria composition drives primary resistance to cancer immunotherapy in renal cell carcinoma patients. Eur Urol. 2020;78:195–206.

19. McCulloch JA, Davar, D, Rodrigues, RR, Badger, JH, Fang, JR, Cole, AM, Balaji, AK, Vetizou, M, Prescott, SM, Fernandes, MR et al. Intestinal microbiota signatures of clinical response and immune-related adverse events in melanoma patients treated with anti-PD-1. Nat Med. 2022;28:545–556.

20. Matson V, Gajewski TF. Dietary modulation of the gut microbiome as an immunoregulatory intervention. Cancer Cell. 2022;40(3):246–248. doi: 10.1016/j.ccell.2022.02.014.

21. Hakozaki T, Richard C, Elkrief A, Hosomi Y, Benlaïfaoui M, Mimpen I, Terrisse S, Derosa L, Zitvogel L, Routy B, et al. The gut microbiome associates with immune checkpoint inhibition outcomes in patients with advanced non–small cell lung cancer. Cancer Immunol Res. 2020;8(10):1243–1250. doi: 10.1158/2326-6066.CIR-20-0196.

22. Gunjur A, Shao Y, Rozday T, Klein O, Mu A, Haak BW, Markman B, Kee D, Carlino MS, Underhill C, et al. A gut microbial signature for combination immune checkpoint blockade across cancer types. Nat Med. 2024;30(3):797–809. doi: 10.1038/s41591-024-02823-z.

23. Derosa L, Iebba V, Silva CAC, Piccinno G, Wu G, Lordello L, Routy B, Zhao N, Thelemaque C, Birebent R, et al. Custom scoring based on ecological topology of gut microbiota associated with cancer immunotherapy outcome. Cell. 2024;187(13):3373–3389. e16. doi: 10.1016/j.cell.2024.05.029.

24. Fidelle M. A microbiota-modulated checkpoint directs immunosuppressive intestinal T cells into cancers. Science. 2023;380: eabo2296.

25. Antoniotti C, Rossini D, Pietrantonio F, Catteau A, Salvatore L, Lonardi S, Boquet I, Tamberi S, Marmorino F, Moretto R, et al. Upfront FOLFOXIRI plus bevacizumab with or without atezolizumab in the treatment of patients with metastatic colorectal cancer (AtezoTRIBE): a multicentre, open-label, randomised, controlled, phase 2 trial. Lancet Oncol. 2022;23(7):876–887. doi: 10.1016/S1470-2045(22)00274-1.

26. Sonpavde GP. Primary results of STRONG: an open-label, multicenter, phase 3b study of fixed-dose durvalumab monotherapy in previously treated patients with urinary tract carcinoma. Eur J Cancer. 2022;163:55–65.

27. Plaza Onate F. Updated metagenomic species pan-genomes (MSPs) of the human gastrointestinal microbiota. Recherche Data Gouv. 2024; doi: 10.15454/FLANUP.

28. Le Chatelier E, Almeida, M, Plaza Oñate, F, Pons, N, Gauthier, F, Ghozlane, A. A catalog of genes and species of the human oral microbiota. Recherche Data Gouv. 2023; doi: 10.15454/WQ4UTV.

29. MSPminer: abundance-based reconstitution of microbial pangenomes from shotgun metagenomic data. Bioinformatics. Oxford Academic; https://academic.oup.com/bioinformatics/article/35/9/1544/5106712.

30. Blanco-Míguez A, Beghini, F, Cumbo, F, McIver, LJ, Thompson, KN, Zolfo, M, Manghi, P, Dubois, L, Huang, KD, Thomas, AM et al. Extending and improving metagenomic taxonomic profiling with uncharacterized species using MetaPhlAn 4. Nat Biotechnol. 2023; 1–12. doi: 10.1038/s41587-023-01688-w.

31. Gargari G, Mantegazza G, Taverniti V, Del Bo' C, Bernardi S, Andres-Lacueva C, González-Domínguez R, Kroon PA, Winterbone MS, Cherubini A, et al. Bacterial DNAemia is associated with serum zonulin levels in older subjects. Sci Rep. 2021;11 (1):11054. doi: 10.1038/s41598-021-90476-0.

32. Ma S, Shungin D, Mallick H, Schirmer M, Nguyen LH, Kolde R, Franzosa E, Vlamakis H, Xavier R, Huttenhower C. Population structure discovery in meta-analyzed microbial communities and

inflammatory bowel disease using MMUPHin. Genome Biol. 2022;23(1):1–31. doi: 10.1186/s13059-022-02753-4.

33. Antoniotti C, Rossini, D, Pietrantonio, F, Salvatore, L, Marmorino, F, Ambrosini, M, Lonardi, S, Bensi, M, Moretto, R, Tamberi, S et al. FOLFOXIRI plus bevacizumab and atezolizumab as upfront treatment of unresectable metastatic colorectal cancer (mCRC): updated and overall survival results of the phase II randomized AtezoTRIBE study. JCO. 2023;41:3500–3500.

34. Karcher N, Nigro, E, Punčochář, M, Blanco-Míguez, A, Ciciani, M, Manghi, P, Zolfo, M, Cumbo, F, Manara, S, Golzato, D. et al. Genomic diversity and ecology of human-associated Akkermansia species in the gut microbiome revealed by extensive metagenomic assembly. Genome Biol. 2021;22:209.

35. Akkermansia beyond muciniphila - emergence of new species Akkermansia massiliensis sp. nov. CoLab. https://colab.ws/articles/10.20517%2Fmrr.2024.28.

36. Mora D, Lessor, L, Le, T, Clark, J, Gill, JJ, Liu, M. Complete genome sequence of Klebsiella pneumoniae jumbo phage Miami. Microbiol Resour Announc. 2021;10:e01404–20.

37. Dong N, Yang X, Chan EW-C, Zhang R, Chen S. Klebsiella species: taxonomy, hypervirulence and multidrug resistance. eBiomedicine. 2022;79:103998. doi: 10.1016/j.ebiom.2022.103998.

38. Ghiringhelli F, Bibeau, F, Greillier, L, Fumet, JD, Ilie, A, Monville, F, Laugé, C, Catteau, A, Boquet, I, Majdi, A et al. Immunoscore immune checkpoint using spatial quantitative analysis of CD8 and PD-L1 markers is predictive of the efficacy of anti-PD1/PD-L1 immunotherapy in non-small cell lung cancer. EBioMedicine. 2023;92:104633.

39. Li J, Lin S, Vanhoutte PM, Woo CW, Xu A. Akkermansia muciniphila protects against atherosclerosis by preventing metabolic endotoxemia-induced inflammation in apoe-/- mice. Circulation. 2016;133:2434–2446.

40. Everard A. Microbiome of prebiotic-treated mice reveals novel targets involved in host response during obesity. Isme J. 2014;8:2116–2130.

41. Everard A. Cross-talk between Akkermansia muciniphila and intestinal epithelium controls diet-induced obesity. Proc Natl Acad Sci USA. 2013;110:9066–9071.

42. Karlsson CLJ, Önnerfält J, Xu J, Molin G, Ahrné S, Thorngren-Jerneck K. The microbiota of the gut in preschool children with normal and excessive body weight. Obes (Silver Spring). 2012;20 (11):2257–2261. doi: 10.1038/oby.2012.110.

43. Li J, Zhao F, Wang Y, Chen J, Tao J, Tian G, Wu S, Liu W, Cui Q, Geng B, et al. Gut microbiota dysbiosis contributes to the development of hypertension. Microbiome. 2017;5(1):1–19. doi: 10.1186/s40168-016-0222-x.

44. Depommier C, Everard, A, Druart, C, Plovier, H, Van Hul, M, Vieira-Silva, S, Falony, G, Raes, J, Maiter, D, Delzenne, NM et al. Supplementation with Akkermansia muciniphila in overweight and obese human volunteers: a proof-of-concept exploratory study. Nat Med. 2019;25:1096–1103.

45. Plovier H, Everard A, Druart C, Depommier C, Van Hul M, Geurts L, Chilloux J, Ottman N, Duparc T, Lichtenstein L, et al. A purified membrane protein from Akkermansia muciniphila or the pasteurized bacterium improves metabolism in obese and diabetic mice. Nat Med. 2017;23(1):107–113. doi: 10.1038/nm.4236.

46. Hu X, Zhao Y, Yang Y, Gong W, Sun X, Yang L, Zhang Q, Jin M. Akkermansia muciniphila improves host defense against influenza virus infection. Front Microbiol. 2021;11. doi: 10.3389/fmicb.2020.586476.

47. Wang L, Tang, L, Feng, Y. A purified membrane protein from Akkermansia muciniphila or the pasteurised bacterium blunts colitis associated tumourigenesis by modulation of CD8+ T cells in mice. Gut. 2020;69:1988–1997.

48. Bárcena C, Valdés-Mas, R, Mayoral, P. Healthspan and lifespan extension by fecal microbiota transplantation into progeroid mice. Nat Med. 2019;25:1234–1242.

49. Bian X, Wu, W, Yang, L. Administration of Akkermansia muciniphila ameliorates dextran sulfate sodium-induced ulcerative colitis in mice. Front Microbiol. 2019;10:2259.

50. Liu Q, Lu, W, Tian, F. Akkermansia muciniphila exerts strain-specific effects on DSS-Induced ulcerative colitis in mice. Front Cell Infect Microbiol. 2021;11:698914.

51. Depommier C, Everard, A, Druart, C. Serum metabolite profiling yields insights into health promoting effect of A. muciniphila in human volunteers with a metabolic syndrome. Gut Microbes. 2021;13:1994270.

52. Yonekura S. Cancer induces a stress ileopathy depending on B-adrenergic receptors and promoting dysbiosis that contribute to carcinogenesis. Cancer Discov Candisc. 2021; doi: 10.1158/2159-8290.CD-21-0999.

53. Yachida S, Mizutani S, Shiroma H, Shiba S, Nakajima T, Sakamoto T, Watanabe H, Masuda K, Nishimoto Y, Kubo M, et al. Metagenomic and metabolomic analyses reveal distinct stage-specific phenotypes of the gut microbiota in colorectal cancer. Nat Med. 2019;25(6):968–976. doi: 10.1038/s41591-019-0458-7.

54. Thomas AM. Metagenomic analysis of colorectal cancer datasets identifies cross-cohort microbial diagnostic signatures and a link with choline degradation. Nat Med. 2019;25:667–678.

55. Leung E, Lehnert KB, Kanwar JR, Yang Y, Mon Y, McNeil HP, Krissansen GW. Bioassay detects soluble MAdCAM-1 in body fluids. Immunol Cell Biol. 2004;82(4):400–409. doi: 10.1111/j.0818-9641.2004.01247.x.

56. Lindner S, Miltiadous O, Ramos RJF, Paredes J, Kousa AI, Dai A, Fei T, Lauder E, Frame J, Waters NR, et al. Altered microbial bile acid metabolism exacerbates T cell-driven inflammation during graft-versus-host disease. Nat Microbiol. 2024;9(3):614–630. doi: 10.1038/s41564-024-01617-w.

57. Ruutu T, Eriksson B, Remes K, Juvonen E, Volin L, Remberger M, Parkkali T, Hägglund H, Ringdén O. Ursodeoxycholic acid for the prevention of hepatic complications in allogeneic stem cell transplantation. Blood. 2002;100(6):1977–1983. doi: 10.1182/blood-2001-12-0159.

58. Ruutu T. Improved survival with ursodeoxycholic acid prophylaxis in allogeneic stem cell transplantation: long-term follow-up of a randomized study. Biol Blood Marrow Transpl. 2014;20:135–138.

59. Gut Microbiota–Related Biomarkers in Immuno-Oncology | Annual Reviews. https://www.annualreviews.org/content/journals/10.1146/annurev-pharmtox-061124-102218.